Carbohydrate Polymers 86 (2011) 526–535

Contents lists available at ScienceDirect

Carbohydrate Polymers

journal homepage: www.elsevier.com/locate/carbpol

Enhancement of neural cell lines proliferation using nano-structured chitosan/poly(vinyl alcohol) scaffolds conjugated with nerve growth factor

Fatemeh Mottaghitalab[a,b], Mehdi Farokhi[a,c], Vahid Mottaghitalab[d,*], Mohammad Ziabari[e], Adeleh Divsalar[f], Mohammad Ali Shokrgozar[a,**]

[a] National Cell Bank of Iran, Pasteur Institute of Iran, Tehran, Iran
[b] Department of Nanobiotechnology, Faculty of Basic Sciences, Tarbiat Modares University (TMU), Tehran, Iran
[c] Department of Tissue Engineering and Cell Therapy, School of Advanced Medical Technologies, Tehran University of Medical Sciences, Tehran, Iran
[d] Department of Textile Engineering, Faculty of Engineering, Guilan University, Rasht, Iran
[e] Guilan Science and Technology Park (GSTP), Rasht, Iran
[f] Department of Biological Sciences, Tarbiat Moallem University, Tehran, Iran

ARTICLE INFO

Article history:
Received 17 January 2010
Received in revised form 25 April 2011
Accepted 28 April 2011
Available online 11 May 2011

Keywords:
Neural tissue engineering
Chitosan
Poly(vinyl alcohol)
Nerve growth factor
Electrospinning

ABSTRACT

Chitosan/poly(vinyl alcohol) (CS/PVA) conjugated nerve growth factor (NGF) scaffolds for potential neural tissue engineering purposes were prepared using electrospinning. NGF was incorporated onto the electrospun nanofibers to mimic the biochemical properties of the neural tissue. Upon current protocol, cell proliferation significantly imitates by ECM surface topography, matrix porosity, surface area, and chemical structure of electrospun scaffolds. CS/PVA conjugated NGF scaffolds were further assessed in terms of attachment and proliferation of SKNMC and U373 cell lines. The thermodynamic parameters of binding of NGF on CS/PVA scaffolds and the NGF releasing rate were evaluated. It has been shown that the electrospun CS/PVA conjugated NGF nanocomposite fibers possess high surface-area-to-volume ratio to support the attachment and proliferation rate of both cell types.

1. Introduction

A major challenge in neural tissue engineering is to create an alternative to the autograft by fabricating implantable scaffolds capable of bridging long gaps that will produce results similar to autograft without requiring the harvest of autologous donor tissue. This strategy generally involves the expansion of cell lines in vitro, followed by seeding the cells onto a three-dimensional (3D) biodegradable and biocompatible scaffold that provides structural support and can also act as a reservoir for bioactive molecules such as growth factors. The scaffold gradually degrades with time to be replaced by newly grown tissue from the seeded cells (Archibald, Krarup, Shefner, Li, & Madison, 1991; Hoffman et al., 2004; Noble, Munro, Prasad, & Midha, 1998; Uebersax et al., 2007; Willerth & Sakiyama-Elbert, 2007).

Nowadays, nanofibrous scaffolds are widely used for tissue engineering applications due to the advantages including: (1) large specific surface providing relatively high quantity of cell loading per unit mass, (2) fine porous structure ensuring the accessibility of active sites and high diffusivity necessary for cell attachment and high proliferation rate, and (3) the macroscopic form of nanofibers offering easy recoverability from growth media (Uebersax et al., 2007). Currently, there are three techniques available for the fabrication of nanofibers: electrospinning, self-assembly, and phase separation. Of these techniques, electrospinning is the most extensively studied technique and has also demonstrated the most promising results in terms of tissue engineering applications (Huang, Ge, & Xu, 2007; Reneker & Chun, 1996). In the electrospinning process a high voltage DC electric potential is applied between the end of a capillary tube and a collector. When the applied electric field overcomes the surface tension of the droplet, a charged jet of polymer solution is ejected and nanofibers are collected on a target (Fong & Reneker, 2001; Frenot & Chronakis, 2003; Subbiah, Bhat, Tock, Parameswaran, & Ramkumar, 2005). Fig. 1 illustrates the electrospinning set up. The availability of a wide range of natural and synthetic biomaterials has broadened the scope for development of nanofibrous scaffolds, using the electrospinning. In the present study, chitosan (CS) and poly(vinyl alcohol) (PVA) nanofibers have been exploited as scaffolds due to their highly controllable chemical and physical properties (Drury & Moony, 2003; Khademhosseini, Langer, Borenstein, & Vacanti,

* Corresponding author at: University of Guilan, P.O. Box 3756, Rasht, Iran.
** Corresponding author at: Pastour institute, 69, Pasteur Ave., Tehran 13164, Iran. Tel.: +98 21 66492595; fax: +98 21 66492595.
E-mail addresses: motaghitalab@guilan.ac.ir, motaghitalab@yahoo.com (V. Mottaghitalab), mashokrgozar@pasteur.ac.ir (M.A. Shokrgozar).

0144-8617/$ – see front matter © 2011 Elsevier Ltd. All rights reserved.
doi:10.1016/j.carbpol.2011.04.066

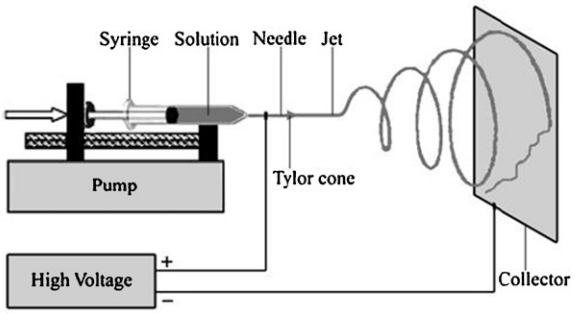

Fig. 1. Electrospinning set up.

2006; Noble et al., 1998). CS is a natural cationic polysaccharide having hydroxyl and amino groups at the equatorial position in the β (1,4)-linked D-glucosamine repeating units (Fig. 2a). It is generally obtained by N-deacetylation of chitin to varying extents (Chuachamsai, Lertviriyasawat, & Danwanichakul, 2008; Costa-Junior, Barbosa-Stacioli, Mansur, Vasconcelos, & Mansur, 2008). CS exhibits properties which are important for biomedical applications such as non-toxicity, physiological inertness, hydrophilicity, remarkable affinity to proteins, and high mechanical strength (Duan, Wu, Li, Yuan, & Yao, 2007; Kumar, 2000; Kurita, 2001). PVA is a non-toxic, water soluble, biocompatible, and biodegradable synthetic polymer which has excellent electrospinnability and also high tensile strength (Fig. 2b) (Chuachamsai et al., 2008; Drury & Moony, 2003; Dutta, Dutta, Chattopadhyaya, & Tripathi, 2004). Combination of PVA and CS polymers could combine the advantage of easy processability of PVA with bio-functionalities of CS (Agarwal, Wendroff, & Greiner, 2008; Uebersax et al., 2007). The use of these scaffolds for neural tissue engineering purposes is often facilitated by specific conjugation of functional targeting molecules such as growth factors to the surface of nanofibers (Agarwal et al., 2008; Koh, Yong, Chan, & Ramakrishna, 2008). In this study, nerve growth factor (NGF) was used in combination with CS/PVA nanofibrous membranes to evaluate the potential of such scaffolds in neural cell lines proliferation. NGF, one of the neurotrophic factors, has been shown to enhance peripheral nerve regeneration and protect neurons from injury-induced death in lesioned peripheral nerves. NGF plays a crucial role in sympathetic and sensory neuron survival and maintenance; to activate their downstream signaling pathways, NGF has high affinity tyrosine kinase receptors, making it a potentially effective therapeutic for the treatment of neurodegenerative disorders (Agarwal et al., 2008; Uebersax et al., 2007; Willerth & Sakiyama-Elbert, 2007). This study aims to prepare and comprehensively investigate the fiber diameter, porosity, physical and chemical properties of electrospun nanofibers composed of CS/PVA blends. Moreover, cell viability was also inspected in order to evaluate the ability of these hybrids to support cell attachment and proliferation. The significance of conjugating NGF with electrospun CS/PVA nanofibers is also addressed.

2. Materials and methods

2.1. Preparation of CS/PVA nanofibrous scaffolds using electrospinning

To fabricate chitosan nanofibrous membranes using the electrospinning process, chitosan (powder, medium molecular weight, degree of deacetylation, DD% = 80%, Sigma–Aldrich, USA) was dissolved in aqueous acetic acid at room temperature with gentle stirring for 2 h to form a 3 wt% homogenous solution. At the same time, PVA (powder, degree of hydrolysis = 80%, degree of polymerization, approximately 2500, Sigma–Aldrich, USA) was dissolved in distilled water at 80 °C with gentle stirring for 4 h to form a 12 wt% homogenous solution. Then, the 3 wt% CS and 12 wt% PVA solutions were gently blended (weight ratio of 1/1.4) up to 1 h and subsequently the air bubbles were totally removed. The reported weight ratio was selected based on two factors including ease of electrospinnability and the nanofiber mechanical stability during cell growth procedure (Shokrgozar, Mottaghitalab, Mottaghitalab, & Farokhi, in press). The mixed solution was placed in a plastic syringe with a 1-mm inner diameter metal needle which was connected to a high voltage power supply. The grounded counter electrode was connected to a collector. Characteristically, electrospinning was performed at 20-kV voltage, 10 cm distance between the needle tip and the collector. It usually took 5 h to obtain a sufficiently thick membrane that could be detached from the collector.

PVA as nanofiber matrix can be readily dissolved in aqueous media leading to scaffold instability. Therefore, CS/PVA nanofiber samples were considered for the next steps using two different approaches. In the first approach, the samples were used for NGF

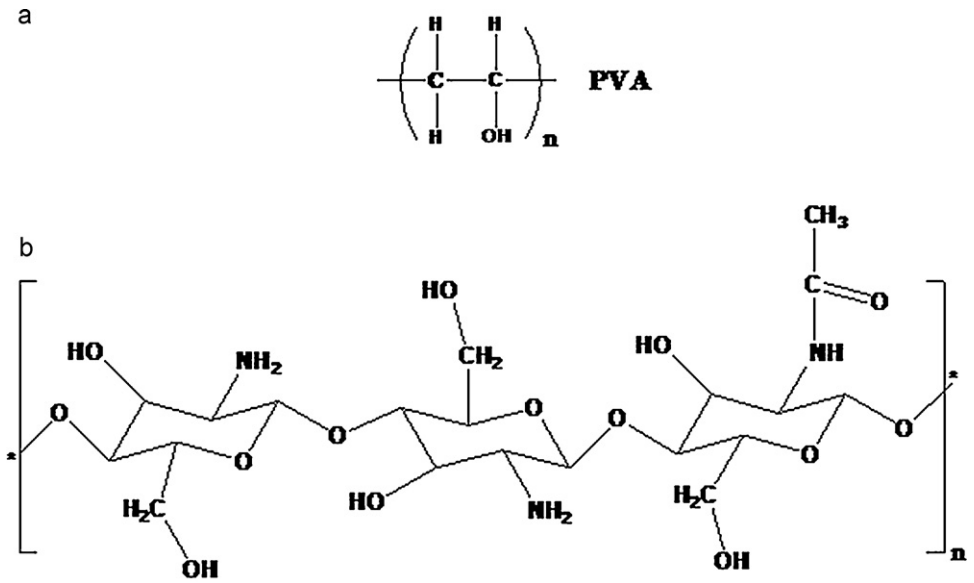

Fig. 2. Chemical structure of Chitosan and PVA (Chuachamsai et al., 2008).

loading without further treatment. In the second approach, removing PVA and enhancing the nanofiber stability in aqueous media through thermal treatment in 180 °C for 1 h was carried out. All composite samples were sterilized with γ-irradiation for 30 min prior to a subsequent cell culturing process.

2.2. Preparation of NGF-loaded CS/PVA nanofibers

CS/PVA nanofibers were prepared as described above; NGF (NGF-β human, Sigma–Aldrich, USA) was dissolved in sterile phosphate-buffered saline (PBS, pH 7.4) to make three different concentrations of 5%, 10%, and 20% of NGF solutions. The nanofibrous membranes were then immersed in NGF solutions for 24 h at 4 °C for the conjugation process.

2.3. The extraction of nanofibers

The extraction of samples for the indirect test was carried out according to the ISO 10993-5 states (Chew, Mi, Hoke, & Leong, 2007). Consequently, all membranes with the surface area of 1 cm^2 were soaked in 1 ml of culture medium (RPMI 1640) in falcon tube and were incubated at 37 °C for 3, 7, and 14 days for cell viability assays.

2.4. Cell cultures

U373-MG (Human glioblastoma-astrocytoma; National Cell Bank of Iran, NCBI) and SKNMC (Human neuroblastoma; National Cell Bank of Iran, NCBI) cell lines were cultured in RPMI 1640 (Biowhittaker, Belgium) with 10% fetal bovine serum (FBS; Sigma–Aldrich, USA) and were incubated at 37 °C with 5% CO_2. The cells were sub-cultured twice per week and were utilized for between 4 and 8 passages.

3. Characterization

3.1. Scanning electron microscopy (SEM) of nanofibers

The morphology of the electrospun CS/PVA nanofibers was assessed by scanning electron microscopy (SEM; Zeiss, Germany). The microscope was attached to a dispersive energy spectrometer (EDS). The images were obtained using an accelerating voltage of 20 kV. The deposited foil was cut into small pieces and attached to a brass stub with carbon tape. All samples were then coated with a gold sputtering device before being investigated under the scanning electron microscope. The porosity of CS/PVA nanofibers was determined using image processing (Ziabari, Mottaghitalab, & Haghi, 2008a; Ziabari, Mottaghitalab, & Haghi, 2008b; Ziabari, Mottaghitalab, & Haghi, 2008c) and fiber diameter distribution was measured by adjusted distance transform method (Ramires, Romito, Cosentino, & Milella, 2001; Ziabari, Mottaghitalab, McGovern, & Haghi, 2007; Ziabari et al., 2008a,b,c; Ziabari, Mottaghitalab, & Haghi, 2009) from the SEM micrographs.

3.2. Raman spectroscopy

Raman spectroscopy was performed to monitor structural changes in CS/PVA nanocomposites directly without further labeling/modification or denaturing of the target. Raman images were taken with an Almega Thermo Nicolet Dispersive Raman Spectrometer using a short working distance 100× objective and with resolution of 4 cm^{-1}. The laser source used was a second harmonic 532 nm of a Nd:YLF laser to avoid excessive fluorescence in the Raman signal.

3.3. Isothermal titration calorimetry (ITC)

ITC was used to evaluate the interaction between NGF and CS based on thermal effects to characterize energetic processes quantitatively (Saboury, 2006). The ITC experiments were performed with a 4-channael commercial microcalorimetric system (Thermal activity monitor 2277, thermostatic, Sweden). Each channel is a twin heat-conduction calorimeter where the heat-flow sensor is a semiconducting thermopile (multi-junction thermocouple plates) positioned between the vessel holders and the surrounding heat sink. The insertion vessel was made from stainless steel. NGF (5 mM) was injected using a Hamilton syringe into the calorimetric titration vessel including a stirrer, which contained 2 ml CS/PVA nanocomposites extraction solution (0.5 mM). The heat of NGF binding on CS was measured with automatic cumulative injections. The thermal effect of each injection was calculated by the "thermometric Digitam 3″ software program.

3.4. NGF releasing study

NGF-conjugated CS/PVA nanocomposites were immersed in PBS solution (pH 7.4) at 37 °C. At each time interval, the solution was collected and replaced with fresh PBS. The collected PBS solutions were stored in −20 °C for later analysis. The amount of NGF in collected PBS solution was measured using Sandwich ELISA following the manufacturer's protocol. Firstly, flat-bottom 96-well polystyrene plates (Nalge Nunc, Roskilde, Denmark) were coated with 50 μl NGF capture antibody solution and the wells were blocked with blocking solution containing a solution of 1% BSA (w/v), 5% sucrose, 0.05% NaN3 in PBS (50 μl/well) for 2 h in 37 °C. Secondly, 50 μl aliquots of NGF test solutions were added to each well after washing the wells twice with TBST (PBS with 0.05% Tween 20) and were incubated in room temperature for 2 h. Thirdly, 50 μl of Anti-NGF-HRP was added to each well and the sample was held for 2 h at room temperature. Finally, TMB (3,3′,5,5′-tetramethylbenzidine) was added as substrate and re-incubated for 30 min and the optical density was measured at 450 nm using an ELISA reader.

3.5. Quantification of viable cells

The cell viability was evaluated using 3-[4,5-dimethyltriazol-2-y1]-2,5-diphenyl tetrazolium bromide (MTT) as a substrate. Briefly, 2×10^4 cells were seeded on matrices within a 96-well plate. The cells were incubated at 37 °C in humidified atmosphere containing 5% CO_2. After 24 h incubation, the culture medium was replaced with 100 μl/well extraction solution of nanofibrous membranes and incubated at 37 °C and 5% CO_2 for 24 h. Finally, the solution extracted from the membranes was removed carefully and was replaced with 100 μl/well MTT solution (Sigma–Aldrich, USA) and re-incubated for 4 h. After that, isopropanol solution (Sigma–Aldrich, USA) was added to the plates in order to dissolve the formazan crystals and was incubated for more 15 min. After slow shaking for an extra 15 min, the absorbance was measured at 570 nm using ELISA reader. Moreover, TPS (Tissue Culture Polystyrene) and CS/PVA nanocomposites without NGF were used as control groups in order to evaluate the potential of composite samples in cell growth and proliferation.

3.6. Cell attachment study

In order to evaluate the attachment of the cell on CS/PVA conjugated NGF nanofibrous membranes, 2×10^4 cells/sample were seeded on the surface of matrices containing different percentages of NGF under the sterile condition. To make a primary attachment, the cells were seeded on the surfaces of membranes under the

slightest amount of the culture medium and standard cell culture conditions for 4 h. After 4 h, 2 ml RPMI 1640 supplemented with 10% FBS was added to each well of a 24-well culture plate and then the plates were incubated at 37 °C and 5% CO_2 for 1,3,7, and 14 days. The culture medium was changed every three days. Two control groups were considered: the composites without NGF as composite control (positive control) and TPS as negative control. After the time intervals, the cells were detached from substrates with 0.25% trypsin/EDTA (Sigma, UK) in PBS for 5 min at 37 °C. The cells were then washed using the culture medium. After preparing a mixture of cell suspension with 0.2% trypan blue solution (1:1; v/v) the count of viable cells were gauged by a light microscope (Zeiss, Germany). CS/PVA nanocomposites without NGF were used as composite control.

3.7. Scanning electron microscopy (SEM) of nanocomposites cultured with cells

The morphology of proliferating cell on nanocomposites was studied using SEM. The U373 and SKNMC cells at a density of 2×10^4 were seeded on the surface of the nanocomposites in the 24-well culture plate. The plates were incubated at 37 °C with 5% CO_2 for 7 days. After 7 days, Samples were fixed in 4% paraformaldehyde for 15 min and dehydrated with graded concentration (50–100% v/v) of ethanol. Subsequently, they were kept in a hood for air drying and used for SEM observation.

3.8. Statistical analysis

All of the quantitative data were expressed as means ± standard deviation. Statistical comparisons were performed using one-way ANOVA with SPSS 16.0 (SPSS, USA). *P* values of less than 0.05 were considered statistically significant.

4. Results

4.1. Scanning electron microscopy (SEM)

Fig. 3a shows the SEM micrograph of CS/PVA nanofibers. The acquired image represents a very narrow size distribution for the CS/PVA nanofiber which confirms the formation of uniform and continuous web of nanofiber necessary for homogenous cell growth. There were also no heterogeneities in the web of nanofiber regarding to insolubility, immiscibility, and phase segregation. Highly uniform and optically transparent films were obtained. Fig. 3b shows the PSD curve. It is quite trivial that the ratio area of fibers to total area increases as the electrospun webs get denser, thus lowering the porosity to the amount of 54.96 nm. It is seen that decreasing the porosity, O_{50} and O_{95} decrease. Cu also decreases with respect to porosity that is, increasing the uniformity of the pores. The number of pores decreases with the porosity as previously reported (Engel, Michiardi, Navarro, Lacroix, & Planell, 2007; Ziabari et al., 2008a,b,c). The diameter distribution of typical electrospun nanofiber mats is also shown in Fig. 3c. The curved line over the histogram corresponds to the fitted normal distribution. Applying the measurement algorithm on binary SEM image gives a mean and standard deviation of nanofiber diameter, respectively equal to 273 nm and 87 nm. The range of nanofiber diameter and its distribution used in current study produce a robust and quite stable 3D scaffold.

4.2. Raman spectroscopy

The Raman signature attributed to CS/PVA composite nanofiber (Fig. 4) shows a combination of enhanced spectra with significant Raman shift for individual CS and PVA. The Raman spectrum of pure chitosan enhances peaks at 1356 cm^{-1} ($NHCOCH_3$) and at about 1566 cm^{-1} for the in plane deformation of NH_2 group (Vasconcelos, Fávere, Gonçalves, & Laranjeira, 2007). The Raman spectrum of pure PVA showed the absorption peaks at about 3100–3300 cm^{-1} for OH group and at about 1082 for the C=O group. In addition the Raman signature of pure PVA shows strong peak of CH_2 deformation and OH–CH (secondary alcohol association band, respectively at 1440 and 1420). It can be seen that the spectra of linear PVA shows a series of medium intensity bands between 1160 and 1050 cm^{-1} which are clearly assigned to C=O stretch of secondary alcohols on the PVA backbone. In addition there is a weak band at 1050–1000 cm^{-1} attributable to the C=O stretch of primary alcohols on the ends of the polymer chains. After the addition of 85% PVA to give the CS/PVA composite, the absorption peak at 1635 cm^{-1} ($NHCOCH_3$) and at about 1566 cm^{-1} for the NH_2 group decreased but the absorption peak at 1169 cm^{-1} for the C–O–C group increased. Also, the intrinsic (CH_2) stretch band of for pure PVA enhances the Raman shift at 3045 cm^{-1} (Gauthiera et al., 2004). High intensity peak at 1800 cm^{-1} are assigned to the C=O group which is mostly due to the amide group of chitin remaining after deacetylation in chitosan structure. A few medium intensity peaks enhanced between 2800 and 3000 cm^{-1} can be also be attributed to the C–H bond present in both CS and PVA structure.

4.3. ITC

The heats of the macromolecules and ligands interactions (q) in the aqueous solvent systems can be reproduced by the following equation (O'Brien, Chowdhry, & Ladbury, 2001; Rezaei Behbehani & Bull, 2005; Rezaei Behbehani, Divsalar, Bagheri, & Saboury, 2008; Saboury, 2006; Schmitt, Sanchez, Desobry, & Hardy, 1998).

$$q = q_{\max} x'_B - \delta^{\theta}_A (x'_A L_A + x'_B L_B) - (\delta^{\theta}_B - \delta^{\theta}_A)(x'_A L_A + x'_B L_B) x'_B \quad (1)$$

The parameters $\delta^{\theta}_A = (\alpha n + \beta N)^{\theta}_A$ and $\delta^{\theta}_B = (\alpha n + \beta N)^{\theta}_B$ are the indexes of the NGF stability as a result of interaction with CS in the low and high CS concentrations, respectively, with *an* resulting from the formation of a cavity wherein *n* solvent molecules become the nearest neighbors of the solute and βN reflecting the enthalpy change from strengthening or weakening of solvent–solvent bonds of *N* solvent molecules ($N \geq n$) around the cavity ($\beta < 0$ indicates a net strengthening of solvent–solvent bonds). The constants α and β represent the fraction of the enthalpy of water + CS interaction associated with the cavity formation or restructuring, respectively. x'_B can be expressed as follow:

$$x'_B = \frac{p x_B}{x_A + p x_B} = \frac{v}{g} \quad (2)$$

where x_B is the fraction of the CS needed for saturation of the binding sites, and $x_A = 1 - x_B$ is the fraction of unbounded CS. We can express x_B fractions, as the total CS concentrations divided by the maximum concentration of the CS upon saturation of all NGF as follow:

$$\chi_B = \frac{[CS]_T}{[CS]_{\max}}$$

$$x_A = 1 - x_B \quad (3)$$

where $[CS]_T$ is the total concentration of CS and $[CS]_{\max}$ is the maximum concentration of the CS upon saturation of all NGF. In general, there will be "g" sites for binding of CS per NGF molecule and v is defined as the average moles of bound CS per mole of total NGF. L_A and L_B are the relative contributions of unbound and bound CS to the enthalpies of dilution in with the exclusion of NGF and can be

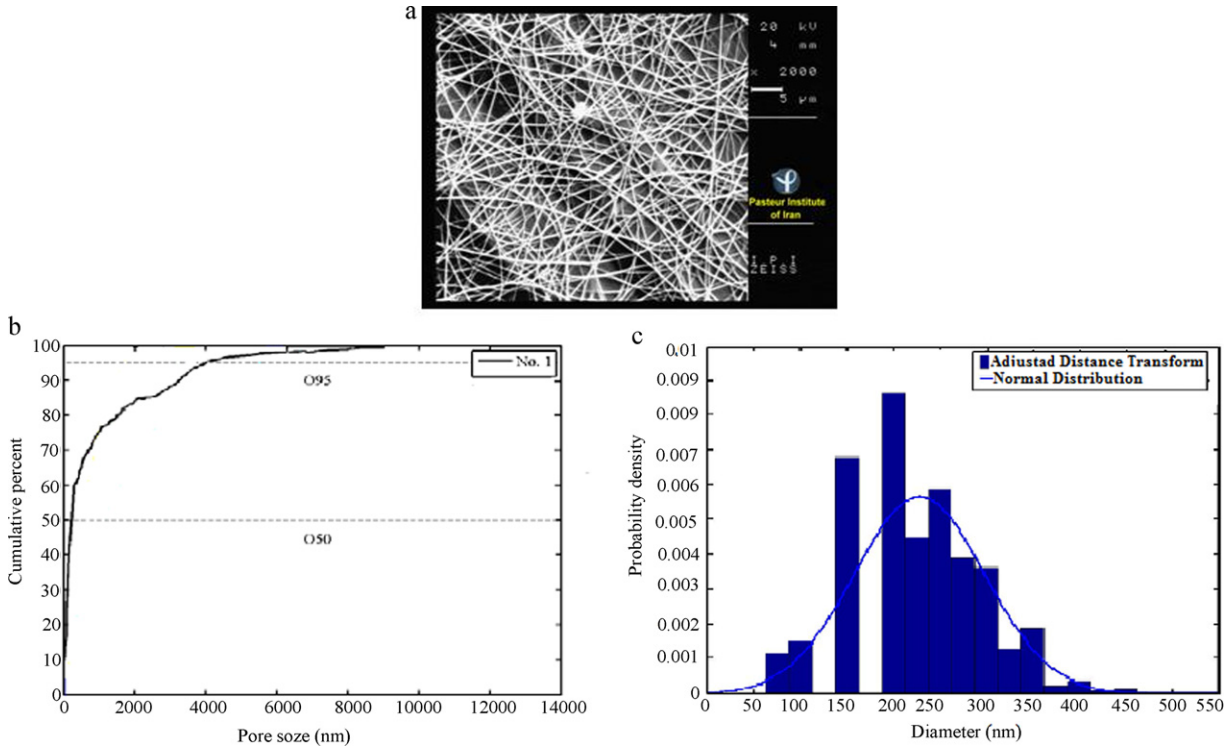

Fig. 3. (a) Scanning electron micrographs of: electrospun CS/PVA nanofibers at 2000× magnification. (b) PSD curve of electrospun CS/PVA nanofiber membranes. (c) Size distribution histogram for electrospun CS/PVA nanofiber membranes.

calculated from the enthalpies of dilution of CS in buffer, ΔH_{dilut}, as follows:

$$L_A = \Delta H_{dilut} + x_B \left(\frac{\partial \Delta H_{dilut}}{\partial x_B} \right) \qquad L_B = \Delta H_{dilut} - x_A \left(\frac{\partial \Delta H_{dilut}}{\partial x_B} \right) \quad (4)$$

The heats of NGF and CS interactions were fitted to Eq. (1) over the entire CS concentrations. In the procedure, the only adjustable parameter (p) was changed until the best agreement between the experimental and calculated data was approached. $(\alpha n + \beta N)^{\theta}$ and δ_B^{θ} parameters have been also optimized to fit the data. The optimized $(\alpha n + \beta N)^{\theta}$ and δ_B^{θ} values are recovered from the coefficients of the second and third terms of Eq. (1). The small relative standard coefficient errors and the high r^2 values (0.9999) support the method. The binding parameters for NGF and chitosan interactions

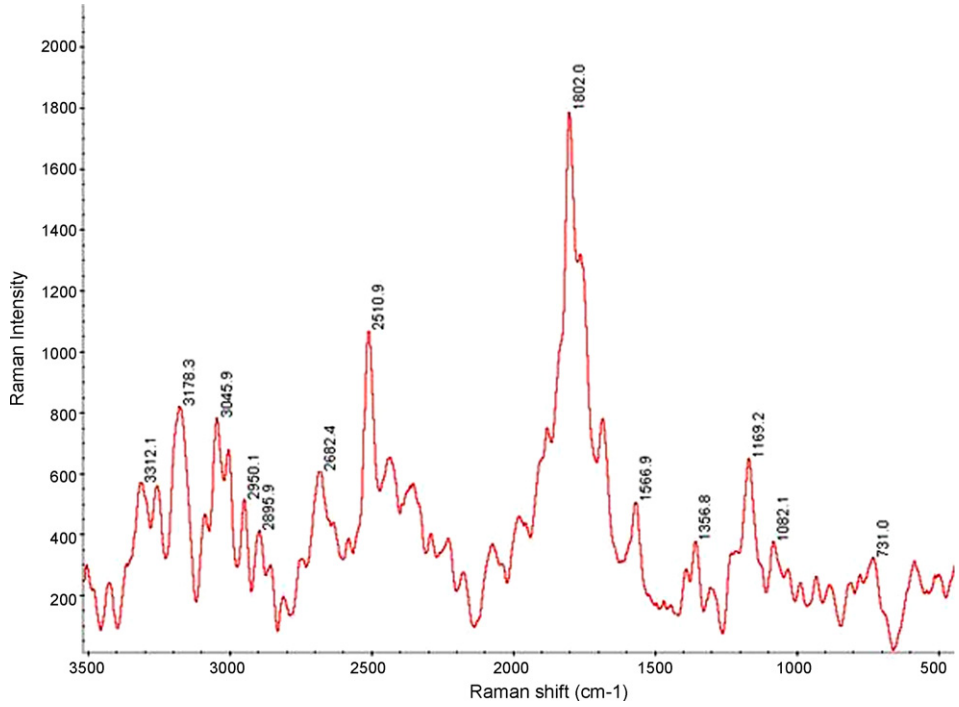

Fig. 4. Raman spectra of PVA nanofiber prior and after chitosan addition.

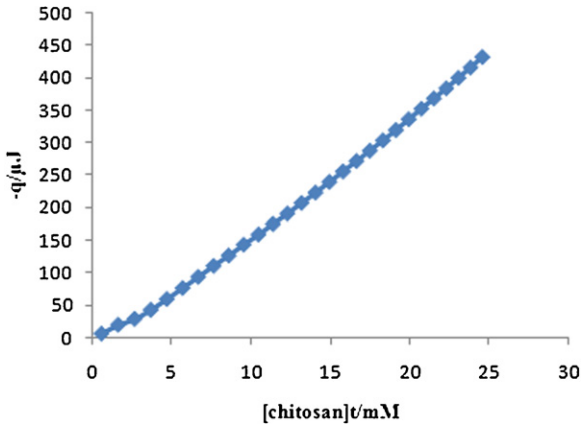

Fig. 5. The heat of NGF binding with chitosan: indicating that in the low and high concentrations of the chitosan, the NGF structure is stabilized, resulting in an increase in its biological activity.

recovered from Eq. (1) are listed in Table 1. $(\alpha n + \beta N)^{\theta}$ value for NGF and CS interaction in first binding site are positive, indicating that in the low concentrations of the CS, the NGF structure was stabilized, resulting in an increase in its biological activity. The negative value of δ_B^{θ} in second binding site indicates that CS destabilizes the NGF in the high CS concentration. As there are two groups of binding sites on NGF, we have introduced the following empirical equation which is the best approach for fitting such a complicated system

$$\frac{(q_{\max 1} - q)}{q_{\max 1}} M_0 + \frac{(q_{\max 2} - q)}{(q_{\max 2} - q_{\max 1})} M_0 = \frac{(q_{\max 1} - q)}{q} L_0 \frac{1}{g_1} - \frac{k_1}{g_1} + \frac{(q_{\max 2} - q_{\max 1} - q)}{F(q_{\max 2} - q_{\max 1}) - q} L_0 \frac{1}{g_2} - \frac{k_2}{g_2} \quad (5)$$

where the F parameter can be defined as follows:

$$F = \frac{q}{q_{\max 1} + q_{\max 2}} \quad (6)$$

A non-linear least squares computer program has been developed to fit data in Eq. (5). The best correlation coefficient ($R^2 \approx 1$) and the least standard deviations (SD $\approx 10^{-6}$ or better) are good support for the use of Eq. (5). The binding parameters recovered from Eq. (5) (K_1, K_2, g_1 and g_2) were listed in Table 1. The curve in Fig. 5 shows the conjugation between NGF and chitosan. Also, the association constants calculated for the NGF-CS suggest high affinity CS-NGF binding, compared to the other strong ligand–macromolecule complexes (Divsalar, Bagheri, Saboury, Mansoori-Torshizi, & Amani, 2009). Therefore, the prepared scaffold would be an ideal structure for further release studies.

Table 1
Binding parameters for chitosan and NGF interaction. $p = 1$ indicates that the binding is non-cooperative in two groups of binding sites. The positive value of $(\alpha n + \beta N)^{\theta}$ indicate that the stability of NGF been increased as a result of its interaction with chitosan.

Parameters	First binding sites	Second binding sites
p	1	1
g_i	2.000 ± 0.001	6.000 ± 0.002
K_d/mM	270.200 ± 0.123	749.000 ± 0.334
q_{max}/μJ	−249.400 ± 0.708	−492.300 ± 1.399
$(\alpha n + \beta N)^{\theta}$	1.66 ± 0.04	–
$(\alpha n + \beta N)^{\theta}$	–	−0.66 ± 0.03

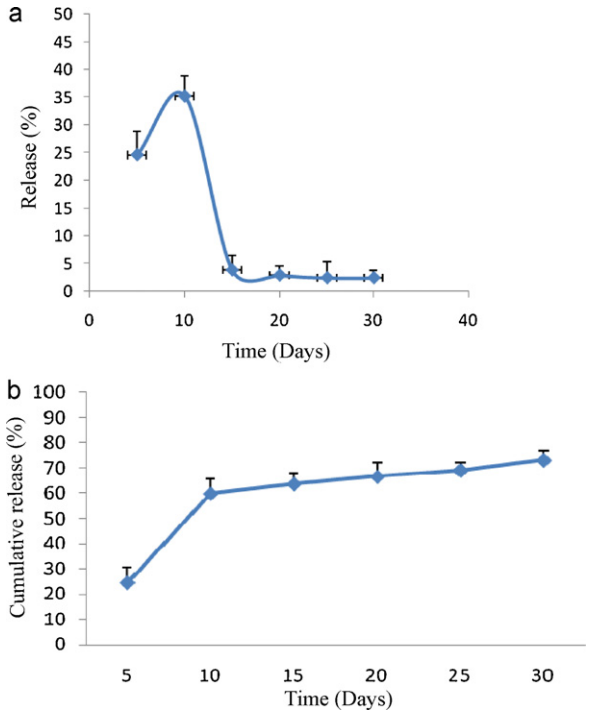

Fig. 6. (a) The NGF releasing curve. (b) In vitro accumulative release (%) of NGF from CS/PVA nanocomposites, 1 cm × 1 cm.

4.4. NGF release study

The amount of NGF released from CS/PVA nanofibrous membranes was analyzed by Sandwich ELISA (enzyme-linked immunosorbent assay) and the test extended for 30 days. The maximum release was about 55% in the 10th day. At the end of day 30, 78% of the total NGF was released. The releasing curve shows two distinct parts with different slopes which reflects the two different releasing mechanisms. The daily release rates are shown in Fig. 6a. At the first 5 days, 24% NGF in average was released from CS/PVA matrices and reached to 35% in average in day 10. As are shown in Fig. 6b, the percentage of cumulative release of NGF from CS/PVA membranes at the first 5 days is about 26% and reached to about 60% in average in the 10th day. After this time, the amount of released NGF was approximately constant.

4.5. Quantification of viable cell

Cell viability was measured using the MTT assay which represents the active mitochondrial enzymes in a cell capable of reducing MTT. As shown in Fig. 7, CS/PVA nanocomposites exhibited comparable biocompatibility. In general, the proliferation rate of SKNMC and U373 cell lines in nanocomposite extraction solutions with different percentages of NGF was similar to negative (TPS) and positive (composite without NGF) control groups. Although, the result showed that the above cell lines have higher viability on a number of CS/PVA nanocomposites with different characteristics. For instance, in the case of SKNMC cell lines, the samples with 5% and 10% NGF in days 7 and 14 had higher proliferation in comparison to TPS and the composite control. Correspondingly, in the regarding of U373 cell lines, this situation only took place in day 7 for nanocomposite samples with 10% NGF ($P < 0.05$).

4.6. Cell attachment study

Adhesion of cells to biomaterials is a major factor for their biocompatibility and it is postulated that the more compatible the

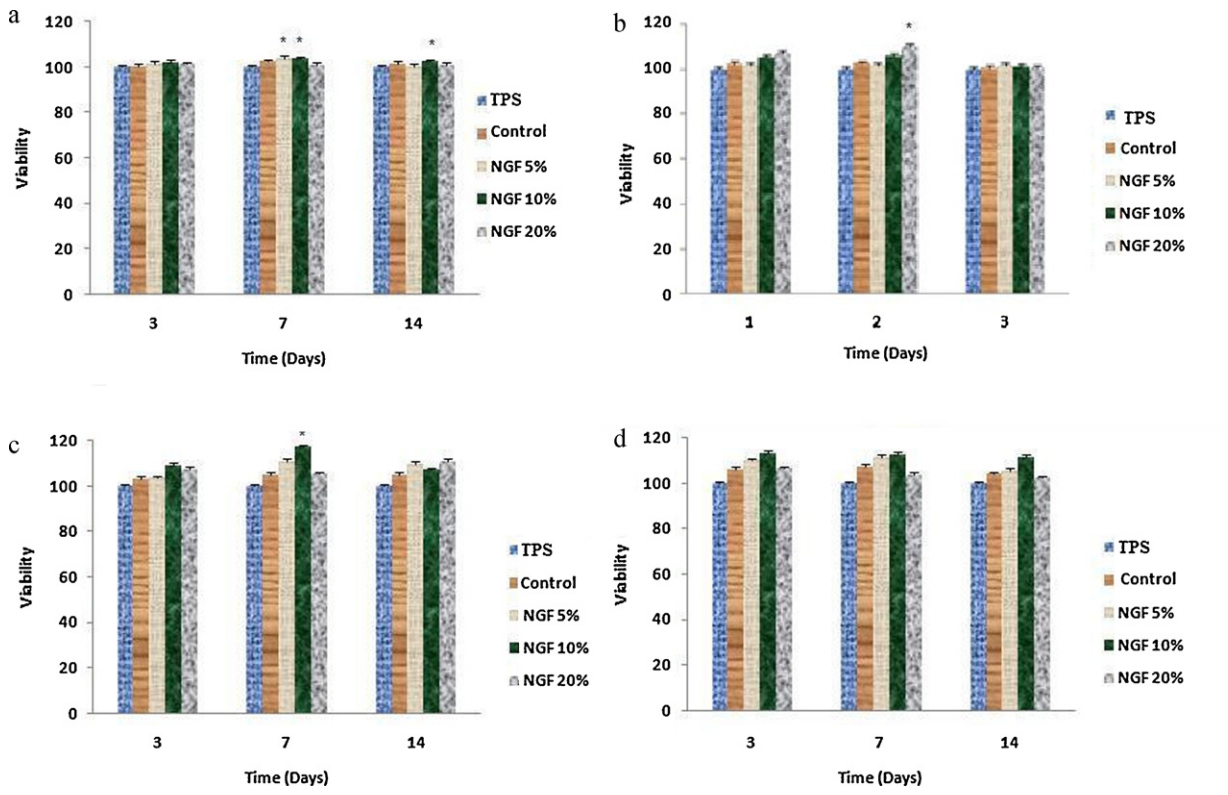

Fig. 7. MTT assay results of the SKNMC and U373 cell lines on CS/PVA nanocomposites at various incubation times and different treatment conditions. CS/PVA nanocomposites without NGF were considered as composite control and tissue culture polystyrene as negative control. (a) Cell proliferation of SKNMC on CS/PVA nanocomposites without treatment. (b) Cell proliferation SKNMC on thermal treated CS/PVA nanocomposites. (c) Cell proliferation of U373 on CS/PVA nanocomposites without treatment. (d) Cell proliferation of U373 on thermal treated CS/PVA nanocomposites. $^{*}P < 0.05$ (compared to the control groups).

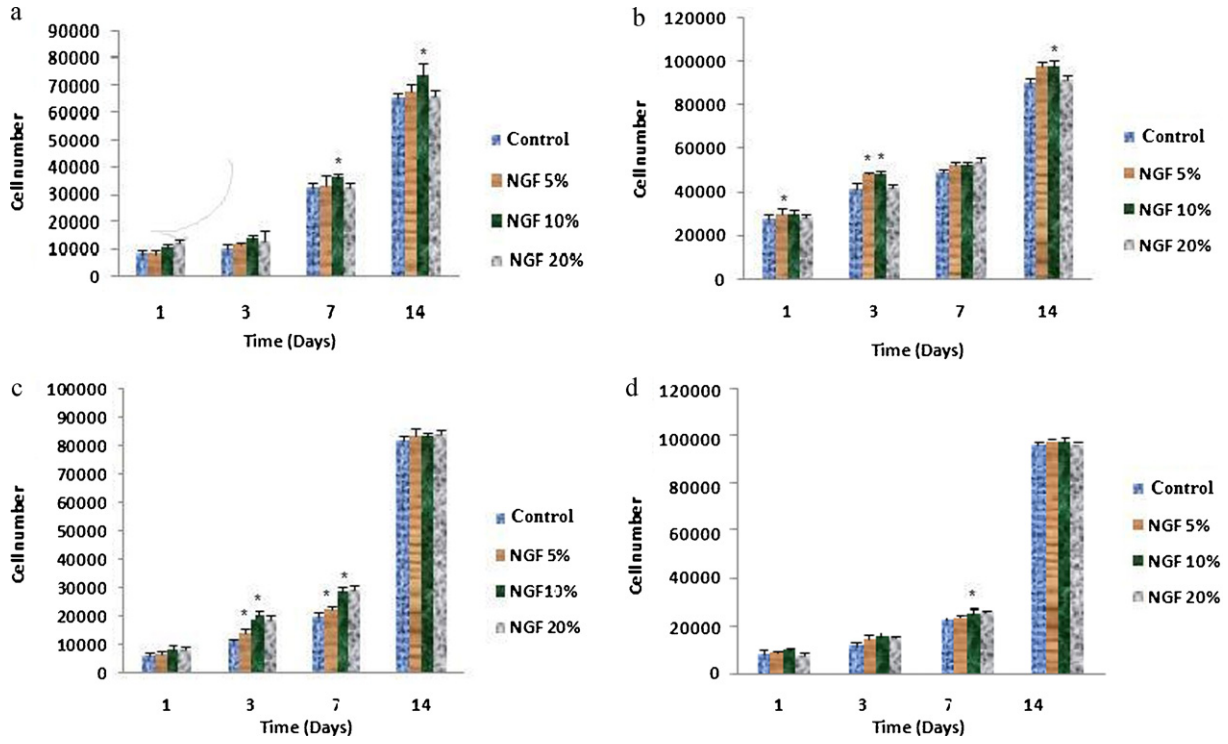

Fig. 8. Attachment of the SKNMC and U373 cell lines on CS/PVA nanocomposites at various incubation times and different treatment conditions. CS/PVA nanocomposites without NGF were considered as composite control. (a) Cell attachment of SKNMC on CS/PVA nanocomposites without treatment. (b) Cell attachment of SKNMC on thermal treated CS/PVA nanocomposites. (c) Cell attachment of U373 on CS/PVA nanocomposites without treatment. (d) Cell attachment of U373 on thermal treated CS/PVA nanocomposites. $^{*}P < 0.05$ (compared to the composite control groups).

surface, the greater the amount of cell attaching. Fig. 8 displays the adhesion of SKNMC and U373 cell lines on electrospun CS/PVA nanocomposites with different characteristics, as well as function of culture time. As are shown in Fig. 8, the cells attached to all the substrates with increasing numbers from day 1 to day 14. It was observed that SKNMC and U373 cell lines could have higher adhesion and proliferation on CS/PVA conjugated NGF nanocomposites in comparison to positive control. Among the samples, nanocomposites with 5% and 10% NGF could enhance proliferation and physical attachment of cells higher than both control groups. However, the cells cultured on the samples with 20% NGF had lower proliferation rate than other nanocomposites.

4.7. Scanning electron microscopy (SEM) of nanocomposites cultured with cells

SEM studies were performed on SKNMC and U373 cells attached to the CS/PVA nanocomposites. As can be seen in Fig. 9, electrospun nanofibers had porous surfaces with appropriate pore size which permit the cells to adhere to the surface of the nanocomposites with suitable morphology. The permeability in CS/PVA nanofibrous membranes is high, allowing the necessary nutrients to reach the seeded cells and thus, high-quality proliferation of both types of cells were observed. It is indicated that the cells could normally be knitted in CS/PVA meshes and created a supporting scaffolds which allow the formation of bio-hybrid tissue that acts as the structural and functional analogue of the original tissue.

5. Discussion

The spinnability of chitosan to form pure and robust nanofibers through the electrospinning process is an extremely challenging area mostly due to polycationic character in an acidic aqueous solution and presence of amino groups in its backbone which increases the surface tension of the solution (Fig. 2b). High electrical force is thus required and particles are often formed during the electrospinning process, probably as a result of the repulsive forces between ionic groups in the CS backbone in acidic solution (Drury & Moony, 2003; Krajewska, 2004; Mansur, Costa-Junior, Mansur, & Barbosa-Stancioli, 2009). Among several attempts for preparation of CS non-woven mat by the electrospinning technique only one group was able to produce CS nanofibers from acetic acid solution (Rboldi, Sampaolesi, Neuenschwander, Cossu, & Mantero, 2005; Shan Zhou, Zhi Yang, & Nie, 2007). The fabricated scaffold, however, did not have the structure to hold and consequently propagate nerve cells. Preliminary results (not shown here) conducted us toward using a supporting biocompatible polymer to resolve current challenge. Poly vinyl alcohol (PVA) is one of promising candidate to make a favorable blend with CS for the cell culture compared to the pure PVA (Berger, Lassner, & Schaller, 1994; Huang et al., 2007). Various aqueous solutions of CS/PVA were prepared, and finally, the spinning solution with a ratio of 15/85 (CS/PVA) retained excellent structural integrity in water.

It is well known that in cell-seeded scaffolds, the response of the cells is affected by the physiochemical parameters of the scaffold, such as surface porosity, diameter distribution, and chemical composition (Engel et al., 2007; Gauthiera et al., 2004; Vasconcelos et al., 2007; Ziabari et al., 2008a,b,c). Most neural cells have sizes on the scale of microns and thus larger pore sizes are needed to allow for cellular infiltration into scaffolds (Ansselin, Fink, & Davey, 1997; Archibald et al., 1991; Noble et al., 1998; Willerth & Sakiyama-Elbert, 2007).

Chemically crosslinked CS/PVA hydrogels with 100–200 μm range size had the ability to support VERO cells attachment and was capable of promoting cellular proliferation (Mansur et al., 2009). However, in recent years a great deal of research has focused on developing fibers with smaller diameters, with the aim of increasing surface area (Agarwal et al., 2008; Chew et al., 2007; Huang et al., 2007; Khademhosseini et al., 2006). The specific characteristics of nanofibers prepared in this study as can be seen in Fig. 3b have a high surface area and highly interconnected porous architectures. They could facilitate the colonization of both cell lines in the scaffold and the efficient exchange of nutrients and metabolic waste between the scaffold and its environment. In addition, the ability of electrospinning process for fiber fabrication in nanoscale (Fig. 3c) may strongly mimics the size scale of fibrous proteins found in natural ECM. In this case, both cell lines were competent to infiltrate into the stable 3D scaffold based on CS/PVA.

Based on Raman spectrum (Fig. 4), the presence of C=O group in CS/PVA blends has intensified the peak enhanced in 1800 cm^{-1} due to amide group of chitin remained after deacetylation in chitosan structure. A few medium intensity peaks also enhance between 2800 and 3000 cm^{-1} that could be attributed to C–H bond present in both CS and PVA structure. Therefore, it can be suggested that the blended polymeric nanofibers could be structured to generate the desired chemical functionality in robust and highly stable scaffolds for consequent cell culturing processes.

As is shown in Table 1, the $p = 1$ indicates that the binding of CS to NGF is non-cooperative in two groups of binding sites. The positive value of $(\alpha n + \beta N)^{\theta}$ indicate that the stability of NGF has been increased as a result of its interaction with chitosan. Also, high values of binding constants (see Table 1) represent the high affinity of chitosan for NGF. A large network of interconnected pores and a high surface area of electrospun nanofiber encourages the in growth tissue to provide local and constant in vitro release of NGF from CS/PVA nanocomposite fibers. The study of release process allows us to understand how NGF cooperates in proliferation process. Two distinct parts were observed in NGF releasing curve (Fig. 6). It is suggested that the initial release of NGF occurs due to the releasing of localized NGF on the surface of the CS/PVA membranes. Subsequent NGF release appears through and control by diffusion process (Chew et al., 2007; Drury & Moony, 2003; Uebersax et al., 2007). It is recommended that using the design adopted in this study for scaffold fabrication, the increase in the surface area provided by the electrospun CS/PVA nanofibers conjugated with NGF for cellular in-growth appears to be the more dominant factor in enhancing neural cells growth and proliferation as compared to CS/PVA matrices without NGF. It is well established that NGF regulates axonal growth in sensory neurons, both regenerative growth in response to injury and collateral sprouting of uninjured nerve terminals (Ansselin et al., 1997; Diamond, Holmes, & Coughlin, 1992; Kimpinski, Campenot, & Mearow, 1997; Lindsay, 1998).

Furthermore, cytotoxicity tests using cell cultures have been applied as the first step in identifying active compounds and for bio-safety testing. The results from cell viability assays as are shown in Fig. 7, the ability of CS/PVA matrices to support cell viability was verified, where the whole set of nanofibrous membranes evaluated exhibited comparable biocompatibility where the cellular proliferation rates of both cell lines were similar or even higher that TPS and control groups. Beyond that, cell proliferation was assessed via the adhesion and spreading test and the general morphology was observed by SEM. These findings could be attributed to the potential of NGF to promote cellular in-growth. It can be noted that the SKNMC and U373 cell lines seeded on the matrix with the good adhesion and spreading morphology required for these cell lines (Fig. 8). Since cellular attachment, adhesion, and spreading belong to the first phase of cell/material interactions, the quality of this phase will influence the proliferation of cells on biomaterial surfaces (Bhattarai et al., 2004). Based on SEM results obtained in this study (Fig. 9a and b), one may attribute the SKNMC and

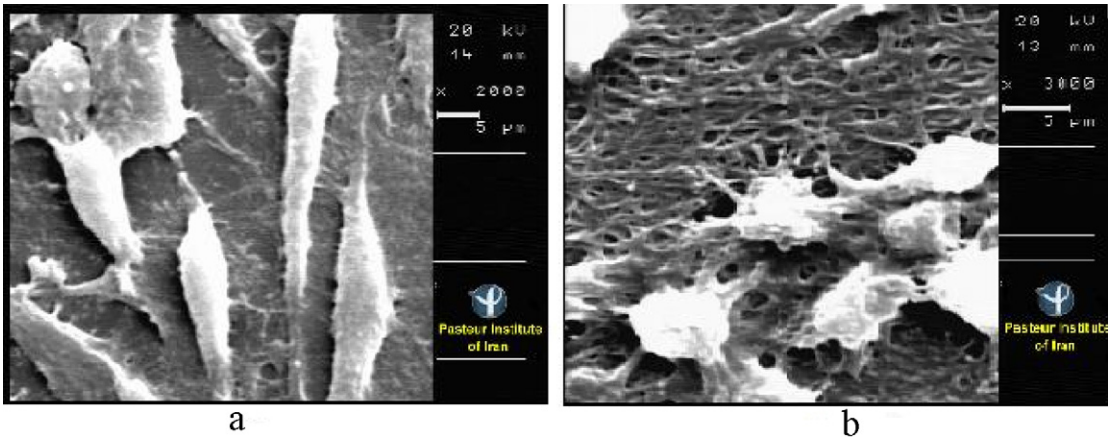

Fig. 9. Scanning electron micrographs of cells proliferated on CS/PVA nanocomposites: (a) U373 cell lines. (b) SKNMC cell lines (magnification: 2000×).

U373 cell spreading and adhesion verified on the CS/PVA matrices to be reliable proof of biocompatibility and non-cytotoxicity of samples. From the results it could be understood that the potential of CS/PVA nanofibrous membranes containing 10% NGF concentration has a greater effect on cellular proliferation in comparison with CS/PVA nanofibrous membranes with 5% and 20% concentrations. Lowering the NGF release rate in days 3 and 14 has decreased the amount of proliferated cells in these days but in day 7 the proliferation rate of cells was higher due to the burst release of NGF in days 5–10. It should be noticed that CS/PVA nanofibrous membranes without NGF, could promote cellular proliferation at the same rate of negative control group (TSP) and the number of cells proliferated on CS/PVA nanofibrous membranes conjugated with NGF was approximately similar to the control group.

Finally, it is demonstrated that CS/PVA nanofibrous membranes conjugated with NGF have considerable biocompatibility without exerting any significant cytotoxic effects which could be used as potential biomaterials for neural tissue engineering applications.

6. Conclusion

Chitosan/poly(vinyl alcohol)-based nanofibers were successfully prepared via electrospinning technique. These nanocomposites provide an optimal microenvironment in terms of porosity, molecular construction, and fiber diameter for the SKNMC and U373 cell lines to maintain relatively high biological activity and stability. To improve the electrospun system, NGF was conjugated to CS/PVA nanocomposites as biochemical cue to promote the survival, growth, and proliferation of both cell lines. Moreover, cytocompatibility, cell viability and preliminary bioactivity assays have given important evidence that all systems evaluated are non-toxic, bio-tolerant and potentially biocompatible. In summary, these novel functional nanocomposites based on CS/PVA conjugated NGF membranes have broadened the number of choices of biomaterials to be potentially used in neural tissue engineering. Nevertheless, once optimization of the scaffold was reached in terms of composition and structure, bio-activation with growth factors were envisaged.

Acknowledgements

The authors thank to the staffs of Cell Bank of Pasteur Institute of Iran for their cooperation and useful consultation. Financial support of National Cell Bank of Pasteur Institute of Iran, University of Guilan and Guilan Science and Technology Park (GSTP) is also acknowledged.

References

Agarwal, S., Wendroff, J., & Greiner, A. (2008). Use of electrospinning technique for biomedical applications. *Polymer*, *49*, 5603–5621.

Ansselin, A. D., Fink, T., & Davey, D. F. (1997). Peripheral nerve regeneration through nerve guides seeded with adult Schwann cells. *Neuropathology Applied Neurobiology*, *23*, 387–398.

Archibald, S. J., Krarup, C., Shefner, J., Li, S. T., & Madison, R. D. (1991). A collagen-based nerve guide conduit for peripheral nerve repair: An electrophysiological study of nerve regeneration in rodents and nonhuman primates. *Composite Neurology*, *306*(4), 685–696.

Berger, A., Lassner, F., & Schaller, E. (1994). The Dellon tube in injuries of peripheral nerves. *Handchirurgie, Mikrochirurgie, Plastische Chirurgie*, *26*, 44–47.

Bhattarai, S. R., Bhattarai, N., Yi, H. K., Hwang, P. H., Cha, D. I., & Kim, H. Y. (2004). Novel biodegradable electrospun membrane: Scaffold for tissue engineering. *Biomaterials*, *25*, 2595–2602.

Chew, S., Mi, R., Hoke, A., & Leong, K. (2007). Aligned protein–polymer composite fiber enhance nerve regeneration: A potential tissue – engineering platform. *Advanced Functional Material*, *17*, 1269–1288.

Chuachamsai, A., Lertviriyasawat, S., & Danwanichakul, P. (2008). Spinnability and defect formation of chitosan/poly vinyl alcohol electrospun nanofibers. *Journal of Science & Technology*, *13*, 24–29.

Costa-Junior, E., Barbosa-Stacioli, E., Mansur, A., Vasconcelos, W., & Mansur, H. (2008). Preparation and characterization of chitosan/poly(vinyl alcohol) chemically crosslinked blends for biomedical application. *Carbohydrate Polymer*, doi:10.1016/j.carbpol. 2008. 11.015

Diamond, J., Holmes, M., & Coughlin, M. (1992). Endogenous NGF and nerve impulses regulate the collateral sprouting of sensory axons in the skin of the adult rat. *Neuroscience*, *12*, 1454–1466.

Divsalar, A., Bagheri, M. J., Saboury, A. K., Mansoori-Torshizi, H., & Amani, M. (2009). Investigation on the interaction of newly designed anticancer Pd(II) complexes with different aliphatic tails and human serum albumin. *Journal of Physical Chemistry B*, *113*, 14035–14042.

Drury, J., & Moony, D. (2003). Hydrogels for tissue engineering: Scaffold design variables and applications. *Biomaterials*, *24*, 4337–4351.

Duan, B., Wu, L., Li, X., Yuan, X., & Yao, K. (2007). Degradation of electrospun PLGA-chitosan/PVA membranes and their cytocompatibility in vitro. *Biomaterial Science*, *18*, 95–115.

Dutta, P. K., Dutta, J., Chattopadhyaya, M. C., & Tripathi, V. S. (2004). Chitin and chitosan: Novel biomaterials waiting for future developments. *Polymer Materials*, *21*, 321–333.

Engel, E., Michiardi, A., Navarro, M., Lacroix, D., & Planell, J. (2007). Nanotechnology in regenerative medicine: The material side. *Trends in Biotechnology*, *26*(1), 39–47.

Fong, H., & Reneker, D. H. (2001). Electrospinning and the formation of nanofibers. In D. R. Salem (Ed.), *Structure Formation in Polymeric Fibers*. Cincinnati: Hanser.

Frenot, A., & Chronakis, I. S. (2003). Nanostructured electrospun network of conducting polymer. *Current Opinion in Colloid and Interface Science*, *8*, 64.

Gauthiera, M. A., Luo, D., Calvet, D., Ni, C., Zhu, X. X., Garon, M., et al. (2004). Degree of crosslinking and mechanical properties of crosslinked poly (vinyl alcohol) beads for use in solid-phase organic synthesis. *Polymer*, *45*, 8201–8210.

Huang, X., Ge, D., & Xu, Z. (2007). Preparation and characterization of stable chitosan nanofibrous membrane for lipase immobilization. *European Polymer Journal*, *43*, 3710–3718.

Khademhosseini, A., Langer, R., Borenstein, J., & Vacanti, J. (2006). Microscale technologies for tissue engineering and biology. *Proceedings of National Academy of Science of the United States of America*, *21*, 2480–2487.

Kimpinski, K., Campenot, R. B., & Mearow, K. (1997). Effects of the neurotrophins nerve growth factor, neurotrophin-3, and brain-derived neurotrophic factor (BDNF) on neurite growth from adult sensory neurons in compartmented cultures. *Neurobiology*, *33*, 395–410.

Koh, H. S., Yong, T., Chan, C. K., & Ramakrishna, S. (2008). Enhancement of neurite outgrowth using nano-structured scaffolds coupled with laminin. *Biomaterials*, *29*, 3574–3582.

Krajewska, B. (2004). Application of chitin- and chitosan-based materials for enzyme immobilizations: A review. *Enzyme Microbial Technology*, *35*, 126–139.

Kumar, M. (2000). A review of chitin and chitosan applications. *Reactive and Functional Polymers*, *46*, 1–27.

Kurita, K. (2001). Controlled functionalization of the polysaccharide chitin. *Progress in Polymer Science*, *26*, 1921–1971.

Lindsay, R. M. (1998). Nerve growth factors (NGF, BDNF) enhance axonal regeneration but are not required for survival of adult sensory neurons. *Neuroscience*, *8*, 3337–3342.

Mansur, H., Costa-Junior, E., Mansur, A., & Barbosa-Stancioli, E. (2009). Cytocpmpatibility evaluation in cell-culture system of chemically crosslinked chitosan/PVA hydrogels. *Material Science and Engineering*, doi:10.1016/j.msec.2008.12.012

Noble, J., Munro, C. A., Prasad, V. A., & Midha, R. (1998). Analysis of upper and lower extremity peripheral nerve injuries in a population of patients with multiple injuries. *Trauma*, *45*(1), 116–122.

O'Brien, R., Chowdhry, B. Z., & Ladbury, J. E. (2001). *A Practical Approach to Protein–Ligand Interactions: Hydrodynamics and Calorimetry*. Oxford: IRL Press.

Ramires, P. A., Romito, A., Cosentino, F., & Milella, E. (2001). The influence of titinia/hydroxyapatite composite coating on the in vitro osteoblast behavior. *Biomaterials*, *22*, 1467–1474.

Rboldi, S. A., Sampaolesi, M., Neuenschwander, P., Cossu, G., & Mantero, S. (2005). Electrospun degradable polyesterurethane membrane: Potential scaffold for skeletal muscle tissue engineering. *Biomaterials*, *26*, 4606–4615.

Reneker, D. H., & Chun, I. (1996). Conducting polymer fibers of polyaniline doped with camphorsulfonic acid. *Nanotechnology*, *7*, 216.

Rezaei Behbehani, G., & Bull, J. (2005). Application of a new method to reproduce the enthalpies of transfer of NaI from water to aqueous methanol, ethanol and iPrOH solvent systems at 289.15 K. *Korean Chemical Society*, *2*, 238–240.

Rezaei Behbehani, G., Divsalar, A., Bagheri, M. J., & Saboury, A. A. (2008). *Journal of the Chemical Solution*, *37*, 1785–1794. doi:10.1007/s10953-008-9322-y

Saboury, A. A. (2006). A review on the ligand binding studies by isothermal titration calorimetry. *Journal of the Iranian Chemical Society*, *3*(1), 1–21.

Schmitt, C., Sanchez, S., Desobry, B., & Hardy, J. (1998). Structure and functional properties of protein–polysaccharide complexes: A review. *Critical Review on Food Science Nutrition*, *38*, 689–753.

Shan Zhou, Y., Zhi Yang, D., & Nie, J. (2007). Preparation and characterization of crosslinked chitosan-based nanofibers. *Chinese Chemical Letters*, *18*, 118–120.

Shokrgozar, M. A., Mottaghitalab, F., Mottaghitalab, V., Farokhi, M. *Biomedical Nanotechnology*, in press.

Subbiah, T. H., Bhat, G. S., Tock, R. W., Parameswaran, S., & Ramkumar, S. S. (2005). Self-assembled honeycomb polyurethane nanofibers. *Applied Polymer Science*, *96*, 557–559.

Uebersax, L., Mattotti, M., Papaloizos, M., Merkle, H., Gander, B., & Meinel, L. (2007). Silk fobroin matrices for the controlled release of nerve growth factor (NGF). *Biomaterials*, *28*, 44–49.

Vasconcelos, H. L., Fávere, V. T., Gonçalves, N. S., & Laranjeira, M. C. (2007). *Reactive and Functional Polymers*, *67*(10), 1052–1060.

Willerth, S., & Sakiyama-Elbert, S. (2007). Approaches to neural tissue engineering using scaffolds for drug delivery. *Drug Delivery*, *59*(4–5), 325–338.

Ziabari, M., Mottaghitalab, V., & Haghi, A. K. (2008a). Distance transform algorithm for measuring nanofiber diameter. *Korean Journal of Chemical Engineering*, *25*, 905–918.

Ziabari, M., Mottaghitalab, V., & Haghi, A. K. (2008b). Simulated image of electrospun nonwoven web of PVA and corresponding nanofiber diameter distribution Korean. *Journal of Chemical Engineering*, *25*, 919–922.

Ziabari, M., Mottaghitalab, V., & Haghi, A. K. (2008c). Evaluation of electrospun nanofiber pore structure parameters. *Korean Journal of Chemical Engineering*, *25*(4), 923–932.

Ziabari, M., Mottaghitalab, V., & Haghi, A. K. (2009). Application of direct tracking method for measuring electrospun nanofiber diameter. *Brazilian Journal of Chemical Engineering*, *26*, 53–62.

Ziabari, M., Mottaghitalab, V., McGovern, S. T., & Haghi, A. K. (2007). A new image analysis based method for measuring electrospun nanofiber diameter. *Nanoscale Research Letters*, *2*, 597–600.